VRN16: A novel PKMYT1 selective kinase inhibitor with wide therapeutic window

Kwangwoo Hwang[1], Seohyun Jo[1], Ho-Soo Lee[1], Youngyi Lee[1], Donghyun Park[1], Songyee Han[1], Kyungah Seo[1], Jiseon Choi[1], Jieun Choi[1], Soochan Kim[1], Jiyeon Kim[1], Donghyuk Seo[1], Younho Lee[1], Yikyung Ko[1], Hyunjong Kwak[1], Ye Ji Son[1], Jeonghun Lee[1], Soyeon Je[1], Hong-ryul Jung[1], Daekwon Kim[1], Sunghwan Kim[1], Jaeyoung Ahn[2]

[1]Voronoi, Inc., Yeonsu-gu, Incheon, South Korea, [2]Voronoi USA, Inc., Boston, MA, USA

AACR American Association for Cancer Research ANNUAL MEETING 2025 CHICAGO

Abstract number: LB436

DO NOT POST

Introduction

- PKMYT1 selectively regulates CDK1 during the G2/M phase transition to prevent mitotic entry in the presence of DNA damage. PKMYT1 inhibition forces cancer cells to prematurely enter mitosis without repairing DNA damage, ultimately leading to cell death.
- CCNE1 amplification is observed in 8% of all solid tumor patients and is particularly prevalent in ovarian cancer (31%), gastric cancer (14%), and breast cancer (8%). CCNE1 amplification drives premature S-phase entry, resulting in genome instability due to DNA replication stress.
- Despite the significant patient population harboring CCNE1 amplification, no targeted therapy has been approved, emphasizing critical unmet medical needs.

Synthetic lethality: CCNE1 amplification with PKMYT1 inhibition leading to cell death

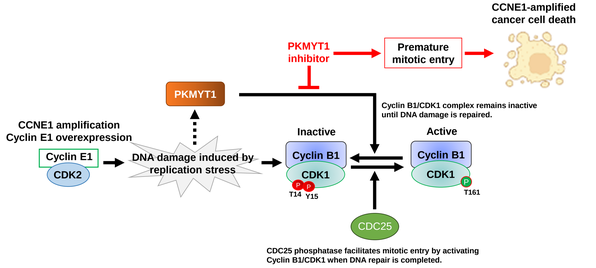

Figure 1. CCNE1 amplification drives premature entry into the G1/S phase, resulting in replication stress and DNA damage. PKMYT1 negatively regulates the Cyclin B1/CDK1 complex by phosphorylating CDK1 at Thr14, thereby preventing mitotic entry until DNA damage is repaired. In CCNE1-amplified cells, inhibition of PKMYT1 overrides this checkpoint, forcing cells into mitosis with unrepaired DNA damage, ultimately leading to cell death.

VRN16: A highly selective PKMYT1 kinase inhibitor

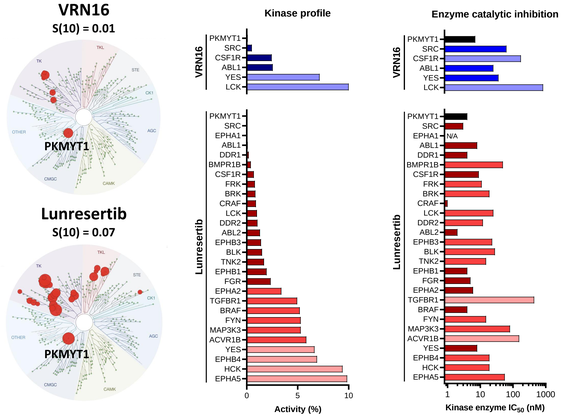

Figure 2. VRN16 kinase selectivity was confirmed at 1 μM by KINOMEscan® (Eurofins). Kinome trees are marked with red circles indicating top 10% hit. Catalytic inhibition potency (IC_{50}) was obtained through HotSpot™ (Reaction Biology), except for PKMYT1, whose catalytic inhibition was measured in-house.

Superior target selectivity and longer target retention

Cell proliferation assay

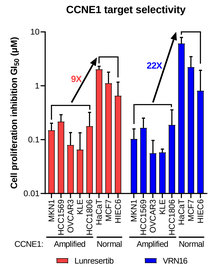

PKMYT1 NanoBRET target engagement assay

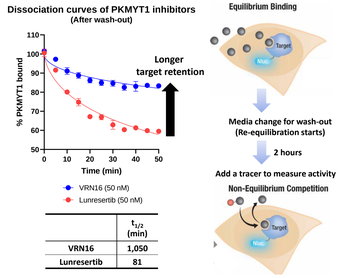

	$t_{1/2}$ (min)
VRN16	1,050
Lunresertib	81

Figure 3. The antiproliferative potency of VRN16 and lunresertib was evaluated in CCNE1-amplified and CCNE1-normal cell lines. VRN16 exhibited a superior CCNE1 target selectivity, as determined by the GI_{50} ratio (CCNE1-normal cell GI_{50} / CCNE1-amplified cell GI_{50}), compared to lunresertib. In the PKMYT1 NanoBRET target engagement assay, VRN16 also exhibited a longer target residence time after compound wash-out than lunresertib.

Safety: Off-target effects of RAF inhibition

Higher RAF sparing ratio based on in vitro profile

Compound	Kinase enzyme IC_{50} (μM) BRAF	GI_{50} (μM) *CCNE1-amplified	**Concentration (μM) at maximum p-ERK level	Relative RAF sparing ratio: Concentration at maximum p-ERK level / GI_{50}
VRN16	0.813	0.100	1.151	6
Lunresertib	0.029	0.123	0.240	1

*CCNE1-amplified cell lines: MKN1, HCC1569, OVCAR3, KLE, and HCC1806 (n≥3)

**Phospho-ERK in cell western assay in HaCaT (n=3)

Paradoxical MAPK pathway activation triggered by RAF inhibition

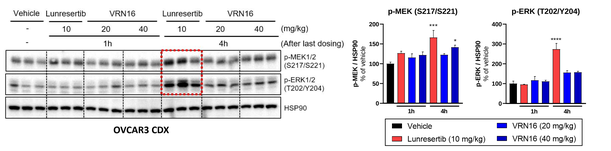

Kinase off-target related adverse events in mice

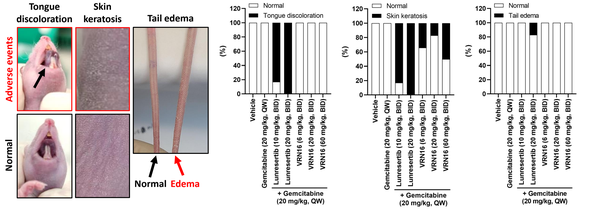

Figure 4. VRN16 demonstrated a higher RAF sparing ratio than lunresertib, as determined by in vitro profiling. In the OVCAR3 CDX model, upregulation of p-MEK and p-ERK signaling, indicative of paradoxical MAPK pathway activation caused by RAF inhibition, was observed in lunresertib-treated tumors. Furthermore, adverse events, including tongue discoloration, keratosis, and edema-potentially related to kinase off-target effects such as RAF inhibition-were predominantly observed in lunresertib-treated groups and not in VRN16-treated groups.

Superior efficacy in CCNE1-amplified tumors

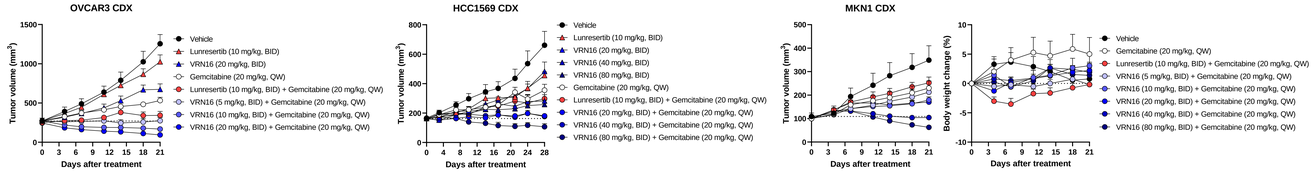

Figure 5. The in vivo efficacy of VRN16 was evaluated in three CCNE1-amplified CDX models (OVCAR3, ovarian cancer; HCC1569, breast cancer; MKN1, gastric cancer). VRN16 demonstrated superior tumor regression efficacy compared to lunresertib when administered in combination with gemcitabine. The body weight change graph indicated that VRN16 was well-tolerated even at a high dose of 80 mg/kg, BID. Each treatment group consisted of six mice (n=6).

Superior target engagement and strong PK-PD correlation

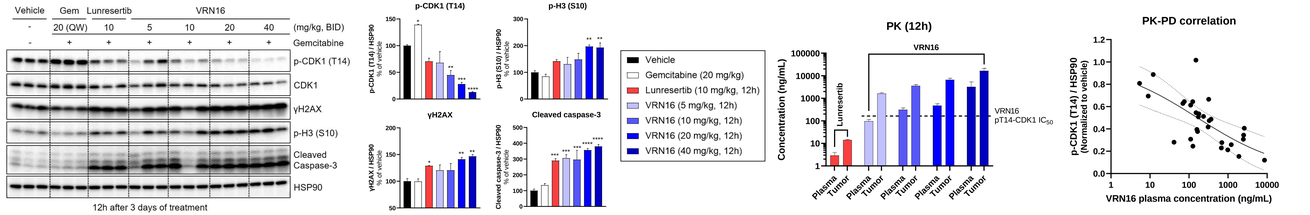

Figure 6. VRN16 showed greater target engagement compared to lunresertib in a dose-dependent manner in the OVCAR3 CDX model. Plasma and tumor PK correlated well with target engagement. The C_{trough} (12h) of VRN16 in OVCAR3 tumors remained above pT14-CDK1 IC_{50}.

Tumor regression efficacy in the ovarian PDX model

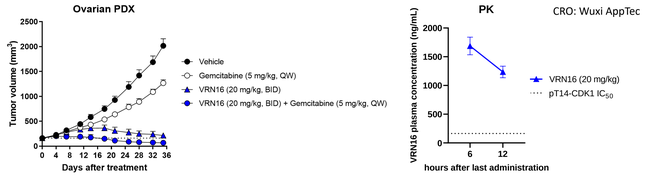

Figure 7. In the ovarian PDX model with high Cyclin E1 expression (data not shown), VRN16 (20 mg/kg, BID) demonstrated tumor regression efficacy when combined with gemcitabine (5 mg/kg, QW). The plasma concentration of VRN16 remained above the pT14-CDK1 IC_{50} level for up to 12 hours after the last adminstration. Each treatment group consisted of six mice (n=6).

Superior efficacy compared to CDK2 inhibitor

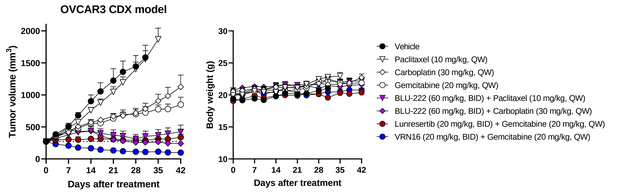

Figure 8. The combination of VRN16 and gemcitabine demonstrated superior efficacy compared to BLU-222, a CDK2 inhibitor targeting CCNE1-amplified cancers, when combined with paclitaxel or carboplatin. Each treatment group consisted of six mice (n=6).

Lower hematopoietic toxicity in gemcitabine combination

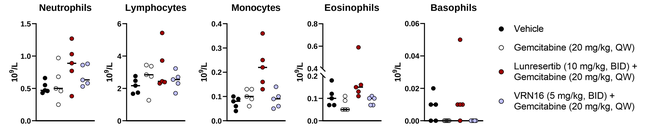

Figure 9. In ICR mice, the CBC analysis was performed after one week of treatment with VRN16 or lunresertib, both in combination with gemcitabine. At equivalent efficacy doses determined for CCNE1-amplified tumor growth inhibition, VRN16 showed no significant hematopoietic toxicity, whereas lunresertib resulted in elevated level of neutrophils, monocytes, eosinophils, and basophils (4 out of 5 WBC components).

Wide therapeutic window

	Efficacy dose	Relative AUC (PK)	MTD (2-week repeated oral dose tox)	Relative AUC (TK)	Relative safety margin (2-week repeated oral dose tox)
VRN16	5 mg/kg, BID (Equivalent efficacy to lunresertib 10 mg/kg, BID)	5	80 mg/kg, QD	81	8
Lunresertib	10 mg/kg, BID	1	20 mg/kg, QD	2	1

Figure 10. VRN16 exhibited a greater safety margin compared to lunresertib. Maximum tolerated doses (MTDs) were determined based on 2-week repeated oral dose toxicity study in ICR mice. Efficacy doses were determined as those achieving equivalent tumor growth inhibition in the CCNE1-amplified CDX models. AUC and safety margin values were reported as relative measures.

Contacts: sunghwan@voronoi.io / ahn@voronoi.io